LANGMUIR

Article

pubs.acs.org/Langmuir

Aqueous Solution-Based Fe_3O_4 Seed-Mediated Route to Hydrophilic Fe_3O_4–Au Janus Nanoparticles

Chenjing Jin, Yun Qu, Minggui Wang, Jie Han,* Yimin Hu, and Rong Guo*

School of Chemistry and Chemical Engineering, Yangzhou University, Yangzhou 225002, Jiangsu, P. R. China

Supporting Information

ABSTRACT: Hydrophilic Fe_3O_4–Au Janus nanoparticles have been synthesized through a facile aqueous solution-based Fe_3O_4 seed-mediated chemical reduction route, where Au nanoparticles can be *in situ* formed on surfaces of PVP-modified Fe_3O_4 nanoparticles by adopting the well-known citrate reduction route. The diameter of Au nanoparticles can be controllably tuned in the range of 3–12 nm by simply changing the initial molar ratio between sodium citrate and auric acid. The as-fabricated hydrophilic Fe_3O_4–Au Janus nanoparticles have shown excellent catalytic performance with high catalytic activity and recyclability due to the synergetic effect between Au and Fe_3O_4 nanoparticles.

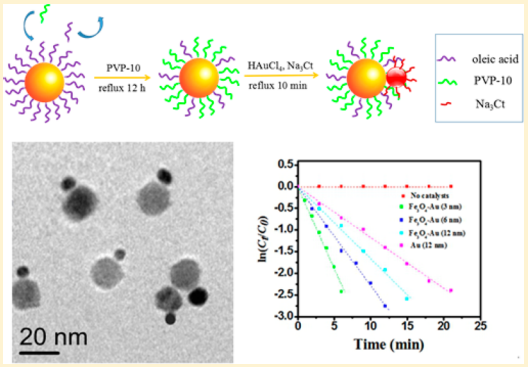

1. INTRODUCTION

Janus nanoparticles (NPs), especially metal–metal oxide NPs, have recently attracted much attention as they have shown novel electronic,[1] optical,[2] and catalytic[3] properties that are not present in the single-component NPs. These new properties can be attributed to the interfacial interactions that may be caused by lattice mismatch between metal and metal oxide support[4] and electron transfer across the interface.[5] In these Janus composite systems, the most well-known is depositing noble metals such as Au, Ag, Pd, and Pt on a magnetic support. Noble metal NPs have been established to play a vital role in many liquid or gaseous catalytic processes.[6−10] However, noble metal NPs with high surface area without a suitable support can easily aggregate in solution, resulting in the loss of their initial catalytic activity. In addition, these catalysts are usually recycled from reaction solution by centrifugation, which could cause the waste of catalysts. Magnetic Fe_3O_4 NPs are chosen to be an ideal support, which can not only prevent the aggregation of noble metal NPs but also can be separated from the reaction mixtures simply by a magnet. Thus, Janus NPs containing noble metal and magnetic Fe_3O_4 NPs have shown high potential in chemical catalysis[1,11,12] and biomedical applications.[13−15]

In previous reports, Fe_3O_4–noble metal Janus NPs were usually prepared through organic solvothermal synthesis by a seed-mediated route using preprepared noble metals with a defined size as seeds for the nucleation of Fe_3O_4 NPs. Severe high temperature control and inert atmosphere protection are essential in this route. For example, Fe_3O_4–Au Janus NPs were prepared by decomposing iron pentacarbonyl ($Fe(CO)_5$) on the surface of the preformed Au NPs synthesized *in situ* by injecting $HAuCl_4$ solution into the reaction mixture at 120–180 °C or premade in the presence of oleylamine. Mixing Au NPs with $Fe(CO)_5$ in octadecene in the presence of oleic acid and oleylamine and heating the mixture to reflux at about 300 °C followed by room-temperature air oxidation leads to the formation of Fe_3O_4–Au Janus NPs.[5,16−18] Similarly, other Fe_3O_4–noble metal Janus NPs, such as Fe_3O_4–Pt,[19] Fe_3O_4–Ag,[20] and Fe_3O_4–Pd,[21] can also be formed through this route. Alternatively, Fe_3O_4–noble metal Janus NPs can also be performed by choosing Fe_3O_4 NPs as seeds for the nucleation of noble metal NPs.[22] However, it should be noted that this route only succeeds in the case of Fe_3O_4–Ag Janus NPs until now. Typical, Fe_3O_4–Ag Janus NPs were prepared by mixing Fe_3O_4 NPs dispersed in organic solution and $AgNO_3$ dissolved in water and agitation by ultrasonication for the formation of a microemulsion with the Fe_3O_4 NPs assembling at the liquid/liquid interface, where Fe^{II} on the NPs acts as catalytic center for the reduction of Ag^+ and nucleation/growth of Ag NPs. In both cases, the obtained Fe_3O_4–noble metal Janus NPs are hydrophobic in nature, which causes the limitation of applications in aqueous solutions. To solve this problem, some strategies have been carried out to transfer the hydrophobic Fe_3O_4–noble metal Janus NPs into aqueous phase. Sun and co-workers[23] functionalized the as-synthesized Fe_3O_4–Au Janus NPs coated with a layer of oleate and oleylamine with poly(ethylene glycol), dopamine, and HS-PEG-NH_2. However, during the surfactant exchange process, dopamine will corrode the Fe_3O_4 NPs. Thus, a size reduction in Fe_3O_4 was observed after surface modification. Ruey[11] selected sodium citrate to wash the oleate and oleyamine on the surface of the Fe_3O_4–Au Janus NPs away. Although the Fe_3O_4–Au Janus NPs could be dispersed in water after washing by sodium

Received: April 3, 2016
Revised: April 21, 2016
Published: April 22, 2016

DOI: 10.1021/acs.langmuir.6b01269
Langmuir 2016, 32, 4595–4601

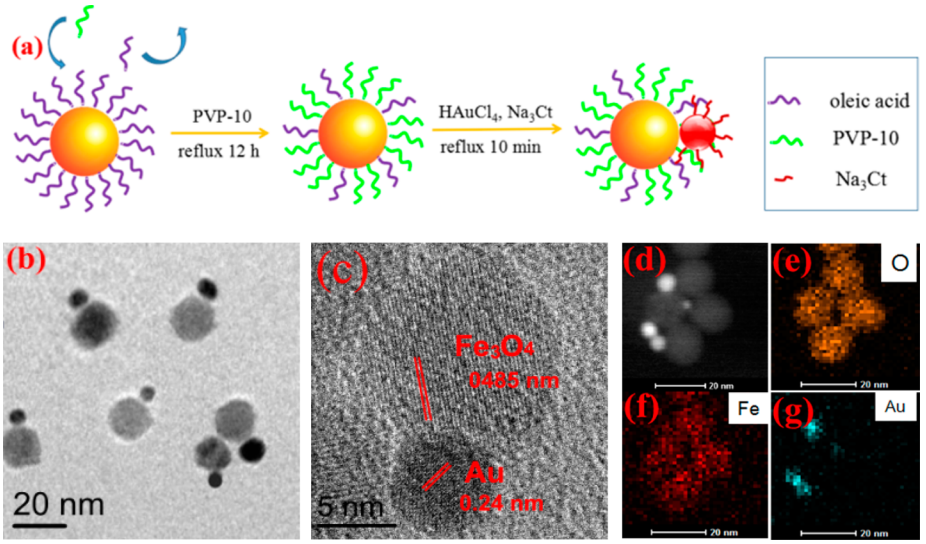

Figure 1. (a) Schematic illustration of the formation of hydrophilic Fe_3O_4–Au Janus NPs. (b) TEM image of hydrophilic Fe_3O_4–Au (6 nm) Janus NPs. (c) HRTEM image of a single hydrophilic Fe_3O_4–Au (6 nm) Janus NP. (d) HAADF-STEM image of l hydrophilic Fe_3O_4–Au (6 nm) Janus NPs. (e–g) EDS maps of several hydrophilic Fe_3O_4–Au (6 nm) Janus NPs.

citrate, the diameter of Fe_3O_4–Au Janus NPs increases to about 500 nm, indicating serious aggregation. Thus, fabricating hydrophilic Fe_3O_4–Au Janus NPs that are monodispersed and stable in aqueous solution through a facile and green way is extremely needed as well as challenging.

Herein, for the first time, we present a facile aqueous solution-based seed-mediated chemical reduction route to prepare hydrophilic Fe_3O_4–Au Janus NPs with remarkable catalytic performance involved in liquid phase catalytic reaction. Different from those previous reports, which choose to first synthesize Fe_3O_4–Au Janus NPs in organic solutions and then to transfer the hydrophobic Fe_3O_4–Au Janus NPs into aqueous phase,[11,23] we start from hydrophilic Fe_3O_4 NPs followed by the *in situ* formation of Au NPs on surfaces of Fe_3O_4 NPs in aqueous solution, resulting in the formation of hydrophilic Fe_3O_4–Au Janus NPs. In this regard, the hydrophilic modification process for Fe_3O_4–Au Janus NPs can be avoided, which often requires complex modification process and encounters severe structure destruction. The well-established citrate reduction route[24] is adopted to synthesize Au NPs due to the simple synthetic conditions and fine-tuned diameter and morphology of Au NPs, which is typically proceeded by sequentially adding auric acid ($HAuCl_4$) solution and sodium citrate (Na_3Ct) solution into boiling water followed by 30 min refluxing. In order to form Fe_3O_4–Au Janus NPs, hydrophilic Fe_3O_4 NPs are introduced into aqueous solution before the addition of Na_3Ct and $HAuCl_4$ precursors. Polyvinylpyrrolidone (PVP) is chosen as the hydrophilic modifier for Fe_3O_4 NPs not only because it is biocompatible, nontoxic, and water-soluble[25−27] but more importantly due to its strong affinity toward noble metal NPs.[28,29] Thus, Au NPs obtained by citrate reduction will preferentially nucleate and grow over the surface of PVP-modified Fe_3O_4 NPs, realizing the formation of hydrophilic Fe_3O_4–Au Janus NPs. The concept for tuning diameter of Au NPs in the citrate reduction route by simply changing the initial molar ratio between Na_3Ct and $HAuCl_4$[30] is also applicable in our case for making hydrophilic Fe_3O_4–Au Janus NPs with Au diameter ranging from 3 to 12 nm. The strategy developed herein is facile, environmentally friendly, and scalable, which provides a highly attractive alternative for making hydrophilic Fe_3O_4–Au Janus NPs. Furthermore, the model catalytic reaction of 4-nitrophenol reduction in the presence of $NaBH_4$ using hydrophilic Fe_3O_4–Au Janus NPs as catalyst demonstrates its remarkable catalytic performance with high catalytic activity and recyclability due to the synergetic effect between Au and Fe_3O_4 NPs.

2. EXPERIMENTAL METHODS

Materials and Methods. 1-Octadecene (ODE, 90%) and polyvinylpyrrolidone (PVP-10, 10 kg mol^{-1}) were purchased from Sigma-Aldrich. Oleic acid, dichloromethane (DMF), dimethylformamide (DCM), auric acid, and all other reagents were obtained from Sinopharm Chemical Reagent Co. Ltd. (China). The water used in this study was deionized and purified through a Millipore system.

Synthesis of Hydrophobic Fe_3O_4 NPs. Hydrophobic Fe_3O_4 NPs were synthesized using a modified method.[31] Iron oleate precursor was first synthesized. Iron chloride (10.8 g) and sodium oleate (36.5 g) were dissolved in a mixture solvent composed of 80 mL of ethanol, 60 mL of distilled water, and 140 mL of hexane. The reaction solution was allowed to stir until the sodium oleate was completely dissolved. Next, the reaction solution was heated to 70 °C and refluxed for 4 h. When the reaction was completed, the upper organic layer containing the iron oleate was washed with distilled water for three times. Hexane was evaporated using a rotary evaporator. The final product of iron oleate is a reddish-brown viscous oil. After that, iron oleate (1.8 g) and oleic acid (0.285 g) were dissolved in 10 g of 1-octadecene at room temperature. After 10 min, the reaction solution was heated to 320 °C at a heating rate of 18 °C/min, and then kept at the temperature for 30 min. The resulting reaction solution containing the NPs was then cooled to room temperature. The NPs were washed three times with a mixture of hexane and acetone by using a centrifuge. The isolated oleic acid-stabilized Fe_3O_4 NPs were stored as 1 wt % dispersion in toluene.

Synthesis of Hydrophilic Fe_3O_4 NPs. The synthesis of PVP stabilized hydrophilic Fe_3O_4 NPs was according to the literature.[32] A dispersion of oleic acid-stabilized Fe_3O_4 NPs in toluene (1.0 mL) was take in a 100 mL round-bottom flask and diluted with DMF (17.5 mL) and DCM (7.5 mL). To this colloidal solution, 300 mg of PVP-10 was added and refluxed at 100 °C for 12 h. The reaction mixture was then added dropwise to diethyl ether to precipitate the PVP-stabilized Fe_3O_4 NPs. The precipitates of PVP-stabilized Fe_3O_4 NPs were washed three times with ethanol by using centrifuge and redispersed in 3 mL of water for further use.

DOI: 10.1021/acs.langmuir.6b01269
Langmuir 2016, 32, 4595−4601

Synthesis of Hydrophilic Fe_3O_4–Au Janus NPs. Deionized water (46 mL) and PVP-stabilized Fe_3O_4 NPs (3 mL) were mixed and vigorously stirred under reflux. After that, a certain amount of sodium citrate solution (10 mg/mL) was added. The resultant solution was stirred until boiling point was reached again. Then, 38.0 μL of $HAuCl_4$ aqueous solution (0.1 mol/L) was added, and the system was refluxed for another 30 min. After cooling to room temperature, the products were magnetic separated and washed with deionized water three times and then dispersed in 10 mL of deionized water for further use.

Instruments. Morphologies were characterized with a transmission electron microscope (TEM, JEM-2100 F) and a high-resolution TEM (HRTEM, Tecnai G2 F30 S-Twin TEM, FEI). The crystal phase was analyzed by X-ray diffraction (XRD) using a Bruker AXS D8 ADVANCE X-ray diffractometer. The products were recorded in the 2θ range from 10° to 85.0° in steps of 0.04° with a count time of 1 s each time. The zeta-potential measurements were carried out using a Zetasizer Nano ZS-90 instrument (Malvern, German). A UV/vis diffuse reflectance spectrophotometer (Cary 5000, Varian) was used to test the optical properties. The phase composition was measured using an Axis Ultra X-ray photoelectron spectroscope (XPS, Kratos Analytical Ltd., UK) equipped with a standard monochromatic Al Kα source ($h\nu$ = 1486.6 eV). The binding energy of the photoelectrons was determined under the assumption that Au has a binding energy of 84.0 eV. Magnetic measurements were carried out using a vibrating sample magnetometer (VSM, EV7, ADE, USA) with a maximum applied continuous field of 10 000 Oe at room temperature.

Catalytic Test. Typically, aqueous solution of $NaBH_4$ (1.0 mL, 1.5×10^{-2} M) and aqueous solution (1.7 mL, 2.0×10^{-4} M) of 4-NP were added into a quartz cell (1 cm path length), followed by adding 20 μL of hydrophilic Fe_3O_4–Au Janus NPs colloidal solution. The progress of the conversion of 4-NP to 4-AP was then monitored via UV–vis spectroscopy by recording the time-dependent adsorption spectra of the reaction mixture with a time interval of several minutes in a scanning range of 200–600 nm at ambient temperature. After each run, the catalysts were collected by a magnet, purified twice with water, and then redispersed in water for usage in the next cycle.

3. RESULTS AND DISCUSSION

Fe_3O_4–Au Janus NPs: Formation Mechanism, Morphology, and Characterization. Figure 1a outlines the general procedures for preparing the hydrophilic Fe_3O_4–Au Janus NPs. First, the hydrophobic Fe_3O_4 NPs were synthesized using a thermolysis process reported previously.[31] Second, the stabilizer oleic acid was replaced by PVP, transferring the hydrophobic Fe_3O_4 NPs into an aqueous phase (Figure S1). Finally, Au NPs obtained by citrate reduction were grown over the surface of PVP-modified hydrophilic Fe_3O_4 NPs due to the existence of PVP, leading to the formation of hydrophilic Fe_3O_4–Au Janus NPs. The aqueous solution of the resulting NPs is stable and can be recovered through simple magnetic separation (Figure S3). As shown in Figure S1a, the oleate-stabilized hydrophobic Fe_3O_4 NPs were spherical and monodispersed. Figure S1b reveals TEM image of hydrophilic Fe_3O_4 NPs after ligand exchange with PVP-10. The as-transferred Fe_3O_4 NPs remain the same morphology and show no obvious aggregation. Figure 1b shows a typical transmission electron microscopy (TEM) image of the as-synthesized hydrophilic Fe_3O_4–Au Janus NPs with Au diameter of about 6 nm. The Au NPs appear black, while the Fe_3O_4 particles present light colored. It is caused by the difference of electron density between Au and Fe_3O_4 NPs as Au has a higher electron density and transmits fewer electrons.[5] Figure 1c displays the typical high-resolution TEM (HRTEM) image of a single hydrophilic Fe_3O_4–Au Janus NP. The interfringe distance is measured to be 0.24 nm for Au and 0.485 nm for Fe_3O_4, corresponding to the (111) plane of fcc structured Au and (111) plane of inverse spinel structured magnetite, respectively. In addition, the high angle annular dark field scanning transmission electron microscope (HAADF-STEM) was further measured to confirm the nanostructure of hydrophilic Fe_3O_4–Au Janus NPs. Different substances show different brightness due to the different intensity of scattered electrons. In addition, the brightness is proportional to the atomic number (Z).[5,33] As shown in Figure 1d, the Au NPs appear brighter due to its higher Z compared to the Fe_3O_4 NPs. The energy-dispersive X-ray spectroscopic (EDS) elemental maps (Figure 1e–g) further confirm the expected Fe_3O_4–Au Janus structure.

Synthesis of Au NPs with tuned diameter by citrate reduction has been well-developed. Frens et al.[30] have proposed that the diameter of the Au NPs can be controllably tuned by simply changing the initial molar ratio between Na_3Ct and $HAuCl_4$. It is interesting to find that the concept is also applicable in our cases as the diameter of Au NPs in hydrophilic Fe_3O_4–Au Janus NPs can also been finely tuned. In this work, the amount of $HAuCl_4$ was set as 38.0 μL (0.1 mol/L). When 1.8 mL of Na_3Ct with a concentration of 10 mg/mL was added to the reaction, 3 nm Au NPs were produced (Figure 2a,c). While the amount of Na_3Ct was decreased to 1.5 and 1.2 mL, 6 nm (Figure 1b) and 12 nm (Figure 2b,d) Au NPs were produced, respectively. However, it should be noted that uniform Fe_3O_4–Au Janus NPs with larger Au diameter cannot be gained if the amount of Na_3Ct is further decreased. Instead, irregular Au NPs with a broad size distribution adsorbed on surface of a small portion of Fe_3O_4 NPs can be observed (Figure S5). In contrast to previous reports on Fe_3O_4–Au Janus NPs where Au NPs should be presynthesized with determined size in oleylamine solution,[5,16–18] the present route shows obvious advantages of green synthesis and facile adjustability in size.

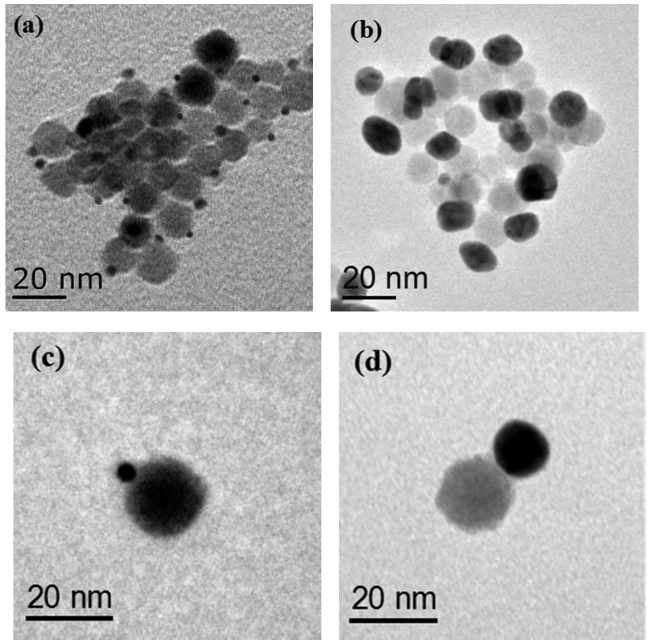

Figure 2. TEM images of typical hydrophilic Fe_3O_4–Au Janus NPs with different size of Au: (a, c) 3 nm; (b, d) 12 nm.

The stability of hydrophilic Fe_3O_4–Au Janus NPs was simply confirmed by storage. As shown in Figure S3, the prepared

DOI: 10.1021/acs.langmuir.6b01269
Langmuir 2016, 32, 4595–4601

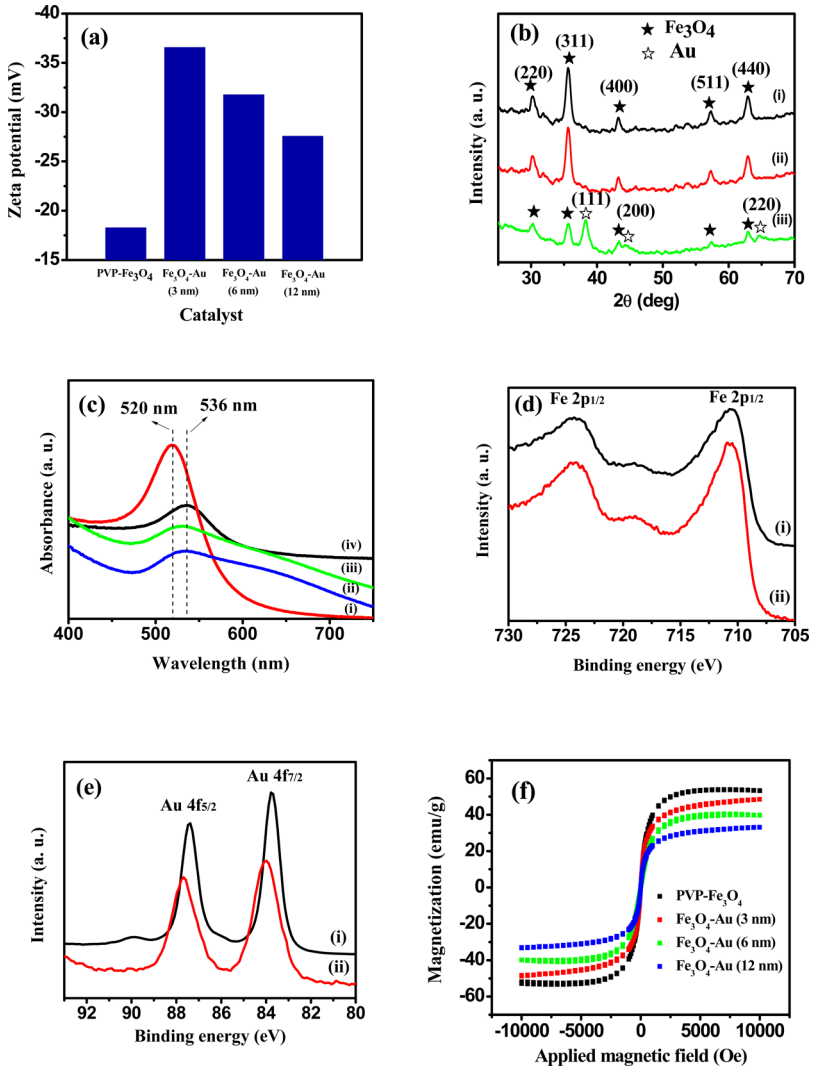

Figure 3. (a) Zeta-potential of PVP–Fe_3O_4 and as-prepared hydrophilic Fe_3O_4–Au Janus NPs. (b) XRD patterns of (i) oleic acid–Fe_3O_4, (ii) PVP–Fe_3O_4, and (iii) hydrophilic Fe_3O_4–Au (6 nm) Janus NPs. (c) UV–vis spectra of (i) 12 nm Au and (ii, iii, iv) hydrophilic Fe_3O_4–Au Janus NPs with Au diameter of 3, 6, and 12 nm, respectively. (d, e) XPS spectra of (c) Fe 2p and (d) Au 4f of hydrophilic Fe_3O_4–Au (6 nm) Janus NPs. (f) Hystersis loops of PVP–Fe_3O_4 and hydrophilic Fe_3O_4–Au Janus NPs.

Fe_3O_4–Au NPs can remain well dispersed in water for at least 12 h. Although there are a few precipitations caused by dipole interactions between magnetic NPs, which pull the adjacent magnetic cores close to each other,[34] they can be redispersed simply by shaking. The stability of the NPs in aqueous solution was further confirmed by zeta-potential measurement. As shown in Figure 3a, the PVP–Fe_3O_4 NPs were negatively charged with a zeta-potential of −18.3 mV. The negative charges were caused by the remaining oleic acid which was not completely replaced by PVP-10. After Au NPs attachment, the surface charge become more negative due to the presence of citrate on Au NPs and the negative charge with a zeta-potential of −36.6 mV, indicating a fine stability of as-formed hydrophilic Fe_3O_4–Au Janus NPs. In addition, as the size of Au NPs increases, the specific surface area decreases correspondingly. This results in decreased adsorptivity of citrate on Au NPs, therefore leading to a decrease in negative charges of the hydrophilic Fe_3O_4–Au Janus NPs.

To characterize the crystal nature of the samples, XRD measurements were carried out on hydrophilic Fe_3O_4–Au Janus NPs. The XRD patterns of Fe_3O_4 NPs before and after ligand exchange are shown in Figure 3b. It reveals that the PVP-stabilized NPs remain their phase after exchange. The observed XRD peaks at 2θ = 30.18°, 35.54°, 43.10°, 57.16°, and 62.78° can be indexed to (220), (311), (400), (511), and (440) planes of fcc Fe_3O_4 (JCPDS 19-0629), respectively. Figure 3b shows representative XRD patterns of hydrophilic Fe_3O_4–Au Janus NPs. Peaks at 38.18°, 44.40°, and 64.68° 2θ can be ascribed to (111), (200), and (220) planes of fcc Au (JCPDS 04-0784), respectively. All the patterns match well with standard Fe_3O_4 and Au power diffraction data, indicating that the synthesis successfully yields single crystalline inverse spinel structured magnetite and fcc structured Au.

Figure 3c displays the UV–vis spectra of the Au and hydrophilic Fe_3O_4–Au Janus NPs. Pure Au particles with size of 12 nm show a surface plasmom resonance peak at 520 nm. Once conjugated with Fe_3O_4 particles, the surface plasmon resonance peak becomes broader and shows absorption at 536 nm. The 16 nm red-shift of surface plasmon resonance spectra of the hydrophilic Fe_3O_4–Au Janus NPs confirms the interface communication between Au and Fe_3O_4 of the Janus NPs.

DOI: 10.1021/acs.langmuir.6b01269
Langmuir 2016, 32, 4595–4601

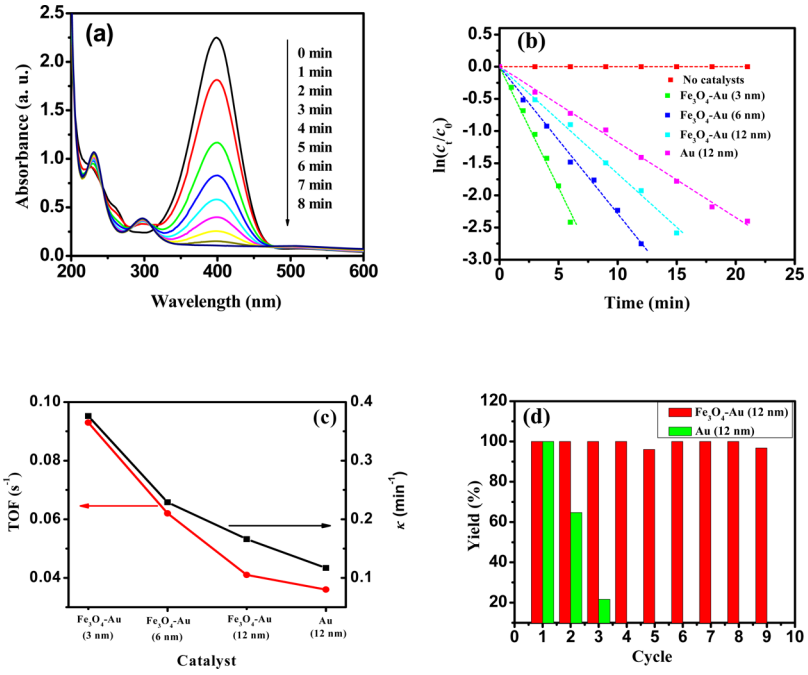

Figure 4. (a) UV−vis spectra showing gradual reduction of 4-NP with hydrophilic Fe_3O_4−Au (3 nm) Janus NPs in the first run. (b) Plot of $\ln(c_t/c_0)$ of 4-NP against time using different catalysts. (c) k and TOF of different catalysts. (d) Synthesis yield of 4-AP in the successive reactions with hydrophilic Fe_3O_4−Au (12 nm) Janus NPs and Au (12 nm) NPs.

XPS was used to characterize the chemical composition and chemical state information on the hydrophilic Fe_3O_4−Au Janus NPs. As shown in Figure S4, the presence of Au for Au NPs, C and N for PVP-10, and Fe and O for Fe_3O_4 NPs confirms the successful formation of hydrophilic Fe_3O_4−Au Janus NPs. Figure 3d reveals the high resolution XPS spectrum of the Fe 2p peaks. The peaks at 711.1 and 724.1 eV are attributed to the binding energy of Fe $2p_{1/2}$. Figure 3e shows the high resolution XPS spectrum of the Au 4f peaks. The doublet peaks at binding energy of 84.0 and 87.7 eV with the splitting of the 4d doublet of 3.7 eV indicate that Au only exists in its metallic state. The Fe 2p peaks and Au 4f peaks of hydrophilic Fe_3O_4−Au Janus NPs were slightly deviated from those of PVP stabilized Fe_3O_4 (711.3 and 724.3 eV) and citrate modified Au (83.7 and 87.4 eV), respectively. It further validates the existence of interface communication between Au and Fe_3O_4.

The magnetic properties of the as-prepared NPs were investigated using VSM. As shown in Figure 3f, the magnetization curves of PVP−Fe_3O_4 and all the hydrophilic Fe_3O_4−Au Janus NPs with different sizes of Au show no remanence or coercivity at room temperature, indicating their superparamagnetic character. The saturation magnetization of PVP−Fe_3O_4 is 51.84 emu/g. Once conjugated with Au particles, the saturation magnetization decreases to 48.34, 39.96, and 33.04 emu/g for the hydrophilic Fe_3O_4−Au Janus NPs with 3, 6, and 12 nm Au, respectively. Although the saturation magnetization is lower than that of bulk magnetite (90 emu/g), even the lowest value (33.04 emu/g) detected here indicates the easy separation of the as-prepared hydrophilic Fe_3O_4−Au Janus NPs from reaction mixtures with a low magnetic field gradient.

Catalytic Performance. The catalytic reduction of 4-NP to 4-AP in the presence of $NaBH_4$ was chosen as a model reaction to evaluate the catalytic performance of as-formed hydrophilic Fe_3O_4−Au Janus NPs. Figure 4a shows the time-dependent adsorption spectra of this reaction mixture in the presence of Au−Fe_3O_4 Janus NPs with 3 nm Au. It is obvious that the peak at 400 nm successively decreases with concomitant increase of a new peak at 300 nm corresponding to the formation of 4-AP. Since the concentration of $NaBH_4$ in the reaction is much higher than the concentration of 4-NP, and the reduction rate could be considered to be independent of the $NaBH_4$ concentration, the reaction was assumed to fit the first-order rate law with respect to the concentration of 4-NP.[35]

Hydrophilic Fe_3O_4−Au Janus NPs with different size of Au were chosen as catalysts for evaluating the effect of catalyst size on catalytic activity. The reduction of 4-NP by $NaBH_4$ does not occur in the absence of catalysts. The reduction of 4-NP into 4-AP was totally finished within 8 min by using the Fe_3O_4−Au Janus NPs with 3 nm Au (Figure 4a), while 12 and 18 min were taken by using Fe_3O_4−Au Janus NPs with 6 and 12 nm Au as catalysts, respectively (Figure S5). For comparison, pure Au NPs modified by citrate (12 nm in size) were also used as the catalyst. It takes more than 20 min to finish the reaction. The concentration of 4-NP at time t and time 0 are noted as c_t and c_0, respectively. The linear relation of $\ln(c_t/c_0)$ versus time is observed for Fe_3O_4−Au Janus NPs catalysts, indicating that the reduction reaction follows the pseudo-first-order kinetics (Figure 4b). The apparent rate constant (k) is estimated to be 0.376, 0.229, and 0.166 min^{-1} by using hydrophilic Fe_3O_4−Au Janus NPs with 3, 6, and 12 nm Au as catalysts, respectively. It suggests that the smaller the Au NPs are the faster reaction rate they show. When pure Au NPs with size of 12 nm are observed as the catalyst, the rate constant is estimated to be 0.117 min^{-1}. In comparison hydrophilic Fe_3O_4−Au (12 nm) Janus NPs and pure Au (12 nm) NPs as catalysts, the k value for hydrophilic Fe_3O_4−Au (12 nm) Janus NPs is about twice higher than that of Au NPs. In addition, the hydrophilic Fe_3O_4−Au Janus NPs catalysts show excellent catalytic performances in terms of high TOF compared to pure Au NPs (Figure 4c). In another control, hydrophilic Fe_3O_4 NPs were added alone instead of hydrophilic Fe_3O_4−Au Janus NPs, and the concentration of 4-NP was almost unchanged (Figure

DOI: 10.1021/acs.langmuir.6b01269
Langmuir 2016, 32, 4595−4601

S6), which eliminates the possibility of catalytic activity of hydrophilic Fe_3O_4 NPs. As a result, it is safe to state that conjugating Au with Fe_3O_4 NPs can greatly enhance the catalytic efficiency of Au NPs. It is believed that the improvement of catalytic efficiency of as-prepared particles is due to the synergetic effect caused by electron transfer across the interface between Au and Fe_3O_4 NPs,[1,36−38] which was confirmed by UV−vis and XPS analysis.

As the hydrophilic Fe_3O_4−Au Janus NPs show both catalytic and magnetic properties, it can be collected easily after the catalytic reduction. Herein, the recyclability of pure Au NPs and hydrophilic Fe_3O_4−Au Janus NPs with 12 nm Au was observed (Figure 4d). It is found that Au NPs as collected by centrifugation can be reused only three times with an apparent decrease in catalytic efficiency. While for hydrophilic Fe_3O_4−Au Janus NPs, the catalysts can be simply recycled and reused for at least nine successive cycles with stable conversion efficiency of around 100%, indicating their high recyclability and stability in aqueous phase catalytic reaction.

4. CONCLUSION

In conclusion, we have developed for the first time a facile aqueous solution-based seed-mediated chemical reduction route for hydrophilic Fe_3O_4−Au Janus NPs. The diameter of Au NPs can be controllably tuned (3−12 nm) by simply changing the initial molar ratio between Na_3Ct and $HAuCl_4$. The catalytic performance is excellent toward the reduction of 4-nitrophenol in the presence of $NaBH_4$ due to the synergetic effect between Au and Fe_3O_4 NPs. It is believed that the strategy to synthesize hydrophilic Fe_3O_4−Au Janus NPs through colloid solution-based chemical reduction route developed here will open a promising way in depositing other noble metals (Ag, Pt, Pd, etc.) on a magnetic support, which will show high potential in fields such as chemical catalysis and biomedical applications.

■ ASSOCIATED CONTENT

Supporting Information

The Supporting Information is available free of charge on the ACS Publications website at DOI: 10.1021/acs.langmuir.6b01269.

Additional structure and catalytic characterization (PDF)

■ AUTHOR INFORMATION

Corresponding Authors

*E-mail hanjie@yzu.edu.cn (J.H.).

*E-mail guorong@yzu.edu.cn (R.G.).

Notes

The authors declare no competing financial interest.

■ ACKNOWLEDGMENTS

The authors gratefully acknowledge financial support from the National Natural Science Foundation of China (No. 21273004) and the Priority Academic Program Development of Jiangsu Higher Education Institutions. We also acknowledge the technical support received at the Testing Center of Yangzhou University.

■ REFERENCES

(1) Lee, Y.; Garcia, M. A.; Huls, N. A. F.; Sun, S. Synthetic Tuning of the Catalytic Properties of Au-Fe_3O_4 Nanoparticles. *Angew. Chem., Int. Ed.* **2010**, *49*, 1271−1274.

(2) Gu, H. W.; Zheng, R. K.; Zhang, X. X.; Xu, B. Facile One-Pot Synthesis of Bifunctional Heterodimers of Nanoparticles: A Conjugate of Quantum Dot and Magnetic Nanoparticles. *J. Am. Chem. Soc.* **2004**, *126*, 5664−5665.

(3) Costi, R.; Cohen, G.; Salant, A.; Rabani, E.; Banin, U. Electrostatic Force Microscopy Study of Single Au−CdSe Hybrid Nanodumbbells: Evidence for Light-Induced Charge Separation. *Nano Lett.* **2009**, *9*, 2031−2039.

(4) Kwon, K. W.; Shim, M. γ-Fe_2O_3/II−VI Sulfide Nanocrystal Heterojunctions. *J. Am. Chem. Soc.* **2005**, *127*, 10269−10275.

(5) Yu, H.; Chen, M.; Rice, P. M.; Wang, S. X.; White, R. L.; Sun, S. Dumbbell-like Bifunctional Au−Fe_3O_4 Nanoparticles. *Nano Lett.* **2005**, *5*, 379−382.

(6) Orlov, A.; Jefferson, D. A.; Macleod, N.; Lambert, R. M. Photocatalytic Properties of TiO_2 Modified with Gold Nanoparticles in the Degradation of 4-Chlorophenol in Aqueous Solution. *Catal. Lett.* **2004**, *92*, 41−47.

(7) Zeng, J.; Zhang, Q.; Chen, J.; Xia, Y. A Comparison Study of the Catalytic Properties of Au-Based Nanocages, Nanoboxes, and Nanoparticles. *Nano Lett.* **2010**, *10*, 30−35.

(8) Hou, L.; Zhang, Q.; Jérôme, F.; Duprez, D.; Can, F.; Courtois, X.; Zhang, H.; Royer, S. Ionic Liquid-Mediated α-Fe_2O_3 Shape-Controlled Nanocrystal-Supported Noble Metals: Highly Active Materials for CO Oxidation. *ChemCatChem* **2013**, *5*, 1978−1988.

(9) Fang, X.; Liu, Z.; Hsieh, M.; Chen, M.; Liu, P.; Chen, C.; Zheng, N. Hollow Mesoporous Aluminosilica Spheres with Perpendicular Pore Channels as Catalytic Nanoreactors. *ACS Nano* **2012**, *6*, 4434−4444.

(10) Liu, Y.; Goebl, J.; Yin, Y. Templated Synthesis of Nano-structured Materials. *Chem. Soc. Rev.* **2013**, *42*, 2610−2653.

(11) Lin, F.; Doong, R. Bifunctional Au-Fe_3O_4 Heterostructure for Magnetically Recyclable Catalysis of Nitrophenol Reduction. *J. Phys. Chem. C* **2011**, *115*, 6591−6598.

(12) Tuo, Y.; Liu, G.; Dong, B.; Zhou, J.; Wang, A.; Wang, J.; Jin, R.; Lv, H.; Dou, Z.; Huang, W. Microbial Synthesis of Pd/Fe_3O_4, Au/Fe_3O_4 and PdAu/Fe_3O_4 Nanocomposites for Catalytic Reduction of Nitroaromatic Compounds. *Sci. Rep.* **2015**, *5*, 13515.

(13) Jiang, J.; Gu, H.; Shao, H.; Devlin, E.; Papaefthymiou, G. C.; Ying, J. Y. Bifunctional Fe_3O_4−Ag Heterodimer Nanoparticles for Two-Photon Fluorescence Imaging and Magnetic Manipulation. *Adv. Mater.* **2008**, *20*, 4403−4407.

(14) Choi, S. H.; Na, H. B.; Park, Y. I.; An, K.; Kwon, S. G.; Jang, Y.; Park, M.; Moon, J.; Son, J. S.; Song, I. C.; Moon, W. K.; Hyeon, T. Simple and Generalized Synthesis of Oxide−Metal Heterostructured Nanoparticles and their Applications in Multimodal Biomedical Probes. *J. Am. Chem. Soc.* **2008**, *130*, 15573−15580.

(15) Umut, E.; Pineider, F.; Arosio, P.; Sangregorio, C.; Corti, M.; Tabak, F.; Lascialfari, A.; Ghigna, P. Facile Synthesis of Monodispersed Silica-Coated Magnetic. *J. Magn. Magn. Mater.* **2012**, *324*, 2373−2379.

(16) Sheng, Y.; Xue, J. Synthesis and Properties of Au−Fe_3O_4 Heterostructured Nanoparticles. *J. Colloid Interface Sci.* **2012**, *374*, 96−101.

(17) Wei, Y.; Klajn, R.; Pinchuk, A. O.; Grzybowski, B. A. Synthesis, Shape Control, and Optical Prolperties of Hybrid Au/Fe_3O_4 "Nanoflower. *Small* **2008**, *4*, 1635−1639.

(18) Wei, Q.; Xiang, Z.; He, J.; Gao, L. W.; Li, H.; Qian, Z. Y.; Yang, M. H. Size and Morphological Effect of Au−Fe_3O_4 Heterostructures on Magnetic Resonance Imaging. *Biosens. Bioelectron.* **2010**, *26*, 627−631.

(19) Wang, C.; Daimon, H.; Sun, S. Dumbbell-like Pt−Fe_3O_4 Nanoparticles and Their Enhanced Catalysis for Oxygen Reduction Reaction. *Nano Lett.* **2009**, *9*, 1493−1496.

(20) Lopes, G.; Vargas, J. M.; Sharma, S. K.; Béron, F.; Pirota, K. R.; Knobel, M.; Rettori, C.; Zysler, R. D. Ag−Fe_3O_4 Dimer Colloidal Nanoparticles: Synthesis and Enhancement of Magnetic Properties. *J. Phys. Chem. C* **2010**, *114*, 10148−10152.

(21) Jang, Y.; Chung, J.; Kim, S.; Jun, S. W.; Kim, B. H.; Lee, D. W.; Kim, B. M.; Hyeon, T. Simple Synthesis of Pd−Fe_3O_4 Heterodimer Nanocrystals and Their Application as a Magnetically Recyclable

DOI: 10.1021/acs.langmuir.6b01269
Langmuir 2016, 32, 4595−4601

Catalyst for Suzuki Cross-Coupling Reactions. *Phys. Chem. Chem. Phys.* **2011**, *13*, 2512−2516.
(22) Gu, H.; Yang, Z.; Gao, J.; Chang, C. K.; Xu, B. Heterodimers of Nanoparticles: Formation at a Liquid−Liquid Interface and Particle-Specific Surface Modification by Functional Molecules. *J. Am. Chem. Soc.* **2005**, *127*, 34−35.
(23) Xu, C.; Xie, J.; Ho, D.; Wang, C.; Kohler, N.; Walsh, E. G.; Morgan, J. R.; Chin, Y. E.; Sun, S. Au-Fe_3O_4 Dumbbell Nanoparticles as Dual-Functional Probes. *Angew. Chem., Int. Ed.* **2008**, *47*, 173−176.
(24) Turkevich, J.; Stevenson, P. L.; Hillier, J. A Study of the Nucleation and Growth Processes in the Synthesis of Colloidal Gold. *Discuss. Faraday Soc.* **1951**, *11*, 55−75.
(25) Rabin, O.; Perez, J. M.; Grimm, J.; Wojtkiewicz, G.; Weissleder, R. An X-ray Eomputed Tomography Imaging Agent Based on Long-Circulating Bismuth Sulphide Nanoparticles. *Nat. Mater.* **2006**, *5*, 118−122.
(26) Pachon, L. D.; Rothenberg, G. Transition-Metal Nanoparticles: Synthesis, Stability and the Leaching Issue. *Appl. Organomet. Chem.* **2008**, *22*, 288−299.
(27) Johnson, N. J. J.; Sangeetha, N. M.; Boyer, J. C.; van Veggel, F. C. J. M. Facile Ligand-Exchange with Polyvinylpyrrolidone and Subsequent Silica Coating of Hydrophobic Upconverting *β*-$NaYF_4$:Yb^{3+}/Er^{3+} Nanoparticles. *Nanoscale* **2010**, *2*, 771−777.
(28) Tsunoyama, H.; Sakurai, H.; Negishi, Y.; Tsukuda, T. Size-Specific Catalytic Activity of Polymer-Stabilized Gold Nanoclusters for Aerobic Alcohol Oxidation in Water. *J. Am. Chem. Soc.* **2005**, *127*, 9374−9375.
(29) Tsunoyama, H.; Sakurai, H.; Ichikuni, N.; Negishi, Y.; Tsukuda, T. Colloidal Gold Nanoparticles as Catalyst for Carbon−Carbon Bond Formation: Application to Aerobic Homocoupling of Phenylboronic Acid in Water. *Langmuir* **2004**, *20*, 11293−11296.
(30) Frens, G. Controlled Nucleation for the Regulation of the Particle Size in Monodisperse Gold Suspensions. *Nature, Phys. Sci.* **1973**, *241*, 20−22.
(31) Park, J.; An, K.; Hwang, Y.; Park, J. G.; Noh, H. J.; Kim, J. Y.; Park, J. H.; Hwang, N. M.; Hyeon, T. Ultra-Large-Scale Syntheses of Monodisperse Nanocrystals. *Nat. Mater.* **2004**, *3*, 891−895.
(32) Rho, W.; Kim, Y. H. M.; Kyeong, S.; Kang, Y. L.; Kim, D. H.; Kang, H.; Jeong, C.; Kim, D. E.; Lee, Y. S.; Jun, B. H. Facile Synthesis of Monodospersed Silica-Coated Magnetic Nanoparticles. *J. Ind. Eng. Chem.* **2014**, *20*, 2646−2649.
(33) Nellist, D.; Pennycook, S. J. Incoherent Imaging Using Dynamically Scattered Coherent Electrons. *Ultramicroscopy* **1999**, *78*, 111−124.
(34) Ge, J.; Hu, Y.; Zhang, T.; Yin, Y. Superparamagnetic Composite Colloids with Anisotropic Structures. *J. Am. Chem. Soc.* **2007**, *129*, 8974−8975.
(35) Panigrahi, S.; Basu, S.; Pal, T. Synthesis and Size-Selective Catalysis by Supported Gold Nanoparticles: Study on Heterogeneous and Homogeneous Catalytic Process. *J. Phys. Chem. C* **2007**, *111*, 4596−4605.
(36) Liu, Z. P.; Gong, X. Q.; Kohanoff, J.; Sanchez, C.; Hu, P. Supported Effect in High Activity Gold Catalysts for CO Oxidation. *J. Am. Chem. Soc.* **2006**, *128*, 917−924.
(37) Zheng, N. F.; Stucky, G. D. A General Synthetic Strategy for Oxide-Supported Metal Nanoparticles Catalysts. *J. Am. Chem. Soc.* **2006**, *128*, 14278−14280.
(38) Frey, N. A.; Phan, M. H.; Srikanth, H.; Srinath, S.; Wang, C.; Sun, S. Interparticle interactions in coupled Au-Fe_3O_4 Nanoparticles. *J. Appl. Phys.* **2009**, *105*, 07B502.

DOI: 10.1021/acs.langmuir.6b01269
Langmuir 2016, 32, 4595−4601